21, rue d'Artois, F-75008 PARIS
http : //www.cigre.org

CIGRE US National Committee
2017 Grid of the Future Symposium

Simulation of Real-time Demand-response to Support a Residential Distribution Feeder in Microgrid Mode

V. H. AYON
M. N. ROBINSON
A. A. MAMMOLI
University of New Mexico
USA

SUMMARY

In recent years, power distribution systems have experienced an increased penetration of distributed power generation and storage. While numerous systems to control these resources exist today, more advanced management systems will be necessary in the coming years, as more distributed resources continue to be introduced to distribution level systems. Better management is especially crucial to improve the resilience of power delivery during emergency situations, such as in the case where part of the distribution system could island, operating as a microgrid during a blackout to provide service to critical loads. An enhanced capacity to integrate human behavior models with power flow simulators will become essential for designing distribution management systems, as new technology leads to more customer-owned devices that can be used to match generation and load. In this study, a co-simulation between a residential load synthesis framework, a residential demand-response aggregator, and the GridLAB-D distribution system simulator is performed using the FNCS software (Framework for Networked Co-Simulation). The co-simulation is based on a real distribution feeder with a large battery and a distribution-level solar array that supplies power to 1600 residential consumers and a set of critical loads, including a hospital, supermarket, and a water treatment plant. It is used to demonstrate the combined capabilities of the residential load synthesis coupled with demand response behavior and power distribution models.

KEYWORDS
Distribution feeder, microgrid, real-time demand response, co-simulation, customer behavior models.

mammoli@unm.edu

I. INTRODUCTION

Recent advances in technology have led to a decreasing cost of distributed energy systems ranging from utility scale photovoltaic (PV) and battery energy storage systems, to customer-owned rooftop PV, electric vehicles and other small-scale storage systems. A well-coordinated development and implementation of controls to go along with the increased deployment of such systems could lead to multiple advantages. For example, coordinating the action of storage devices at the distribution level could reduce peak load on the substation transformer, allowing deferral of upgrades. Frequency support could be provided to the transmission grid by the ability of a distribution feeder to rapidly respond to load adjustment requests, thereby reducing the likelihood of blackouts or brownouts.

Sections of distribution systems with the ability to function as microgrids, could turn to island mode to provide service to critical loads in the case that a blackout does occur. Furthermore, a well-designed control framework could enable new business models that involve customer engagement to manage residential loads. Despite current standards and guidelines, further research is required in the areas of communications, controls, architecture, and human behavioral models for full deployment of such framework. Research in the human behavioral area is limited due to the difficulty to test new methods in realistic situations. A useful tool to conduct research in this context is a simulator that combines the ability to model electric infrastructure in combination with customer behavior and associated electric loads at the meter and even at the appliance level. Work recently published by the authors of this paper [1] showcases the development of such simulation tool, which integrates the GridLAB-D agent-based distribution system simulation platform [2] with a human-behavior based residential load synthesis model. An enhanced version of this tool, which takes advantage of the Pacific Northwest National Laboratory's FNCS software (Framework for Networked Co-Simulation), is used here to demonstrate how a behavioral model can be used to study the effects of the human factor in distribution level load management with demand response. While models exist that simulate both of these domains, a combined model did not exist prior to the introduction of this co-simulation tool.

II. THE FEEDER MODEL

A. From GIS to GridLAB-D

Circuit 16, one of the feeders of the power distribution network located in Los Alamos, NM, was selected for this study due to its distributed energy resources and the diversity of its loads, as it serves residential, commercial, and critical loads such as water distribution pumps. This feeder, shown in Fig. 1, also hosts a 1 MW photovoltaic (PV) array and a substation-sited battery energy storage system (BESS) composed of a 1 MW / 7.2 MWh NaS battery and a 0.8 MW / 1.2 MWh lead-acid battery. The local municipal utility, Los Alamos Department of Public Utilities (LADPU), maintains a high fidelity model of the Circuit 16 feeder based on accurate equipment specifications and Geographic Information System (GIS) data within WindMil, a power utility software designed to model and analyze electric distribution networks for system planning and operations [3]. This model was translated into a GridLAB-D model using the WindMil export function.

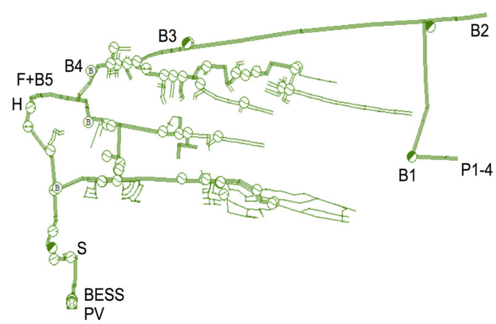

Fig. 1. Configuration of the Circuit 16 feeder, operated by the Los Alamos Department of Public Utilities. Note the presence of water supply well pumps (P1-P4), several pressure booster stations (B1-B5) and a water filter station (F). A 1MW PV array (PV), and 2 MW / 8 MWh battery storage (BESS) are located at the feeder head. Hospital (H) and supermarket (S) loads are also shown. Hundreds of residential loads are distributed at the feeder end nodes.

B. Model validation

The Circuit 16 model is defined with a constant voltage of 66,395 V at the source node, stepped down via a transformer to 7,967 V at the head of the feeder. Power distribution through the feeder takes place via overhead and underground lines with three-phase, bi-phase, and single-phase configurations depending on the type of load served. Fig. 2 illustrates a snapshot of the voltage profile across the

GridLAB-D Circuit 16 model. To assess how PV penetration affects the feeder's voltage profile, a solar generation resource was introduced near the end of a branch (at location B3 as shown in Fig. 1) to represent a 1 MW PV array. As expected, the PV penetration caused the voltage profile across the feeder to rise, for all phases. Also, the voltage increase is highest at the injection point, as seen by inspection of Fig. 2. The case with no PV experienced minimum and maximum voltages of 99.25% and 102.37% of nominal, respectively, while the case with PV experienced a minimum voltage of 100.38% of nominal and a maximum of 102.86% of nominal, confirming the Circuit 16 model meets ANSI C84.1 voltage specifications [4].

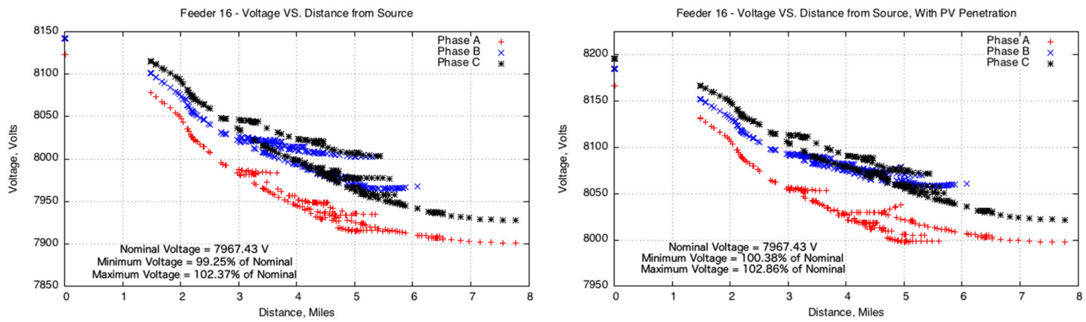

Fig. 2. Voltage on each phase as a function of distance from the head of the feeder. On the left is the case of power injected at the feeder head only. Power injected at feeder head and at the end of a branch by a PV inverter (at B3 for testing purposes, especially noticeable on phase A) is on the right.

III. LOAD SIMULATION

A. Critical infrastructure loads

Distributed energy resources (DERs) at the distribution level, in combination with a distribution management system, can be used to support critical infrastructure in the case of a grid failure. In such emergency situations, a functioning critical infrastructure could enable a 'shelter in place' strategy, and thus limiting the stress imposed on transportation systems and emergency infrastructure during evacuation procedures. Since water, food, and medical care are basic needs for a community, they also considered in this study in an effort to replicate the most realistic load on the feeder as possible. The water system load was developed using pump operation data, provided by LADPU. These pumps contribute to the Los Alamos water supply directly and via a number of water storage tanks. A stochastic approach was used to generate models that simulate the water treatment load associated with Circuit 16. In total, there are four water well pumps and five pressure booster stations included in the Circuit 16 model. The location of the water pumps on the feeder is indicated in Fig. 1, P1-4 and B1-5. Typical pump operation is shown in Fig. 3. Data for a hospital and a supermarket in Santa Fe, NM, a location with very similar climatic conditions, were used as a proxy for the hospital and supermarket loads since high-resolution data for the local establishments are not available. The electric demand for these is also shown in Fig. 3.

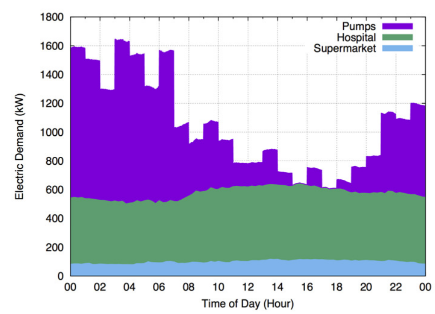

Fig. 3. Critical loads for the Circuit 16 feeder, for July 8, 2016. Note that these loads, while supported by Circuit 16, are shared by the entire Los Alamos community.

B. Statistical residential load synthesis

Residential loads are made up of the aggregated power consumption of individual household appliances ranging from a few Watts to a few kW in consumption. A statistical approach is used to model their operation and interaction with the human users. The use of a specific appliance is described by probability density functions formulated from customer usage patterns and characterized by the number of events per day, their start-time, and duration. Moreover, statistical characterization of each appliance is also associated with a demographic cluster, namely working singles, working couples, families, and retired people to account for the variability in human use patterns and behaviors similar to the method described in the recent work by Fischer et al. [5]. HVAC, water heater, and refrigerator models contain thermodynamic systems; dryers and lights are considered on/off loads; and electric ranges use a Markov-chain approach used by Widén *et al*. for lighting [6]. An example of statistics for electric range operation is shown in Fig. 4.

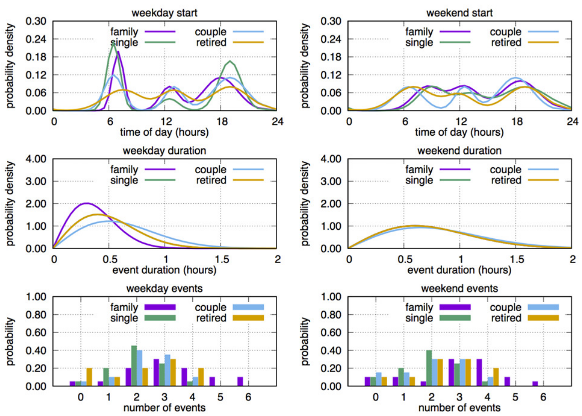

Fig. 4. Probability density functions describing the use of an electric range in terms of start time, load duration, and use events. Note that PDFs are specified for four demographic categories.

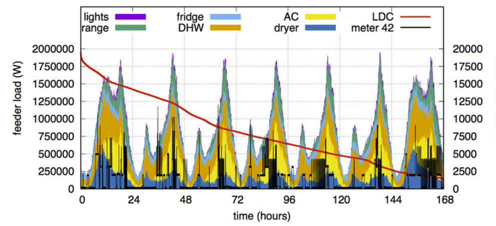

Fig. 5. Total feeder load from 1000 houses, also indicating the aggregated contribution from each appliance. The total load for an individual meter (42) is also shown for comparison.

$$M_s \frac{dT}{dt} = \dot{Q}_L - \dot{Q}_R, \qquad (1)$$

$$\dot{Q}_L = K_1[T_a - T(t)], \qquad (2)$$

$$\dot{Q}_R = \Lambda \times COP \times P_{AC}, \qquad (3)$$

$$\text{if } T(t) < T_L \text{ then } \Lambda = 0, \qquad (4)$$

$$\text{if } T(t) > T_U \text{ then } \Lambda = 1, \qquad (5)$$

The interaction between the load of an appliance and its user is specific to the appliance. For example, the air conditioning system (AC) is described by the temperature setpoints and deadbands set by the user. The interaction between the load and the physical system is described (1)-(3), where M_s is the effective heat capacity of the space, $T(t)$ is the space temperature, T_a is the ambient temperature, t is time, and Q_L and Q_R are the thermal losses from the structure and thermal gain from the air conditioner or heat pump, respectively. K_1 is a function of the building's thermal insulation, COP is the coefficient of performance, P_{AC} is the power of the compressor, and Λ is a state function that indicates whether the air conditioner or heat pump is on or off. In its basic form, the air conditioning or heat pump is controlled by the switching logic in equations (4) and (5) where T_L and T_U are the lower and upper deadbands for the temperature control. A total of five loads are considered including the AC load, refrigerator, heat-pump type water heater, clothes dryer, electric cooking range and lighting. Here, the AC and water-heating units are considered thermostatically controllable loads (TCL) that can be controlled using demand response. Additional information about the operational characteristics of these appliance models is found in [1]. A typical profile of the total feeder load from a collection of 1000 houses is shown in Fig. 5, in comparison with the total load for a single meter for a period of one week. While individual meters display significant variation in time the total feeder load is relatively smooth and predictable. Interestignly, the load duration curve reveals a substantial peak load above 1.5MW that occurs for less than approximately 10% of the time, which could easily be removed by demand response in combination with storage.

IV. INTEGRATION OF GridLAB-D AND LOADS

The GridLAB-D Circuit 16 model was integrated with the residential load generator and the load aggregator using FNCS (Framework for Networked Co-Simulation), a companion software package developed at Pacific Northwest National Laboratories (PNNL) that allows GridLAB-D to interact with other software as co-simulators [8]. In this instance, the FNCS software allows for a co-simulation where the loads are updated by the load generator in synchronicity with GridLAB-D and the load aggregator. Generally, external loads are provided to GridLAB-D through players that read load shapes from static files and apply the load to *load objects*. In this case, the load must evolve in parallel with the GrdiLAB-D simulation in response to demand response directives issued and managed by the aggregator. In this study, the FNCS broker represents the central server that all other simulators will connect to in order to synchronize in time and exchange messages with other simulators [9]. Represented as the interface in Fig. 6, the broker acts as the master clock, simulation synchronizer, and data communicator between the co-simulators. The simulation process is the following:

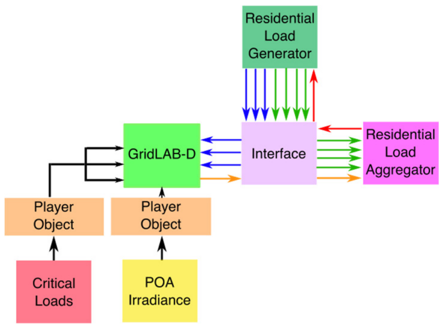

Fig. 6. Block diagram of information flow between FNCS and co-simulators.

1) The co-simulators including GridLAB-D itself, are initialized and they prepare their environment for the first time step, $t=1$. This includes connecting with the FNCS broker and subscribing to publications that will be made by other co-simulators.
2) The FNCS broker receives the status of each simulator and sends the signal to execute for the current time step only when all co-simulators are ready.
3) The simulators receive the signal from the broker and begin by requesting the published values to their subscriptions from the broker. This happens at the beginning of each time step (initial conditions are used for $t=1$).
4) The simulators execute for the current time step, t, and publish their output to the FNCS broker, which then brokers the publications to the respective co-simulator subscription.
5) Steps (2)-(4) are repeated until the simulation ends.

As indicated by step 3, all simulators obtain values to their subscriptions at the beginning of each time step. In this application the load generator simulates a total of 1600 homes aggregated to 594 values that represent the number of residential homes and transformers within the Circuit 16 feeder, respectively. The load generator publishes the TCL status of each home for the aggregator, in addition to the 594 aggregated values for the GridLAB-D Circuit 16 model. In return, the aggregator publishes the control signal for the load generator indicating the demand response directive. Finally, the Circuit 16 model publishes the solar irradiance used by the aggregator to generate the demand response signal, and by the load generator to simulate residential PV. Overall, a total of 2,196 values are transferred between three co-simulators each simulated second.

V. SIMULATION RESULTS

Two cases are considered in this study. The first consists of typical operating conditions in which the utility battery follows a fixed schedule set to charge at night and discharge during peak hours without demand response. In the second case, demand response is used to reduce the duty cycle of the battery.

A. Baseline

Power distribution feeders equipped with DERs such as PV and batteries usually discharge the batteries during peak load hours to reduce the stress on the transformer, while charging takes place at night when wholesale energy cost is low. The results with this mode of operation, shown in Fig. 10, demonstrate that while the residential load consumption of 1600 houses is low during the night, it dominates during the day. Comparing the size of the residential load to the critical loads during the day confirms the potential for aggregated residential demand response as an effective tool to ensure that power is available to serve critical loads. For example, inspection of Fig. 7 indicates that curtailment of air conditioning and domestic water heating loads could reduce the residential load considerably. When operating in island mode, the battery would also have to absorb fluctuations produced by the PV generators. To relieve the battery of some of this stress, the HVAC units are controlled so that in aggregate they follow the output of the PV plant.

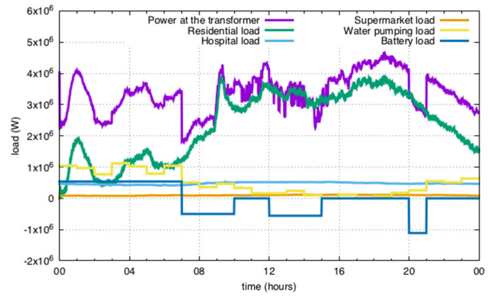

Fig. 7 History of net load at the feeder head, in comparison with critical loads, residential loads and battery charge / discharge on July 18, 2016.

B. Residential demand response

In this study, a residential load aggregator manages the aggregated demand response of the system. In this instance the appliances managed by the aggregator are thermostatically controllable loads (TCL) such as the air conditioner and water-heating units in every home. For example, a 200m^2 house has about 0.15kWh of stored energy per ℃ associated with the air mass alone, coupled with roughly 3kW of power controllable through a home thermostat. The load aggregator aggregates the power consumption of all the AC units based on the state of the units in the system. The total power available to be decreased or increased through demand response depends on the number of units that *ON* and *OFF*, respectively. Instead of controlling each thermostat individually, the load aggregator broadcasts a single signal to all the thermostats in the system. This signal is in the form of a number that represents the probability of an available compressor switching from its current state. Furthermore, each "smart" thermostat decides to switch based on its current state and an internally generated random number. The broadcast signal is generated based on the error between the current power of the TCL system and a desired power setting that can vary dynamically. In other words, the system can be set to follow a static load shape on a schedule set by the utility to reduce the load on a feeder during peak hours, or it can be set to dynamically follow a changing signal. Fig. 8 shows the results from the co-simulation with demand response in which a 400kW TCL system composed of 1600 thermostats follows a solar irradiance profile from 9AM-5PM. The purple line in Fig. 8 shows the aggregated power consumption of the AC units and the yellow curve is obtained by passing the total load through a bandpass recursive time series digital filter [7]. The filtering limits the response to only a specific band of frequencies for comparison with the demand response signal. A closer inspection of the results reveals that the TCL system successfully follows the signal as directed, relieving much of the load from a smoothing battery system.

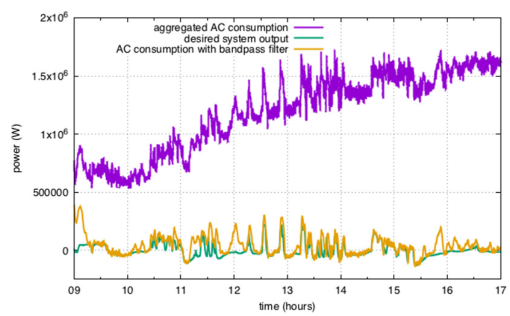

Fig. 8. Aggregated AC demand response successfully following signal from solar irradiance from 9AM-5PM. Total consumption of 1600 AC units in purple, filtered load and signal in yellow and green, respectively.

VI. DISCUSSION & CONCLUSIONS

This work has demonstrated the enhanced capabilities of the FNCS-GridLAB-D co-simulation coupled with human behavioral models to study the impact of the human factor in the management of residential loads using demand response. The results show that an aggregated demand response approach to control thermostatically controllable loads can be used as a resource to support the load on a distribution feeder without compromising the quality of service experienced by the consumers.

BIBLIOGRAPHY

[1] V. Ayon, A. Mammoli, M. Robinson, J.C. Fuller, A. Fisher "Integration of Bottom-up Statistical Models of Loads on a Residential Feeder with the GridLAB-D Distribution system Simulator, and Applications," in *Innovative Smart Grid Technology (ISGT) Europe*, Sep. 2017, Accepted.

[2] D. P. Chassin, J. C. Fuller, and N. Djilali, "Gridlab-d: An agent-based simulation framework for smart grids," Journal of Applied Mathematics, vol. 2014, 2014.

[3] "Milsoft engineering analysis WindMil," https://www.milsoft.com/utilitysolutions/upgrades/-milsoft-engineering-analysis-ea-windmil, accessed: 2017-03-11.

[4] "C84. 1-1982," American National Standard for Electric Power Systems and Equipment Voltage Ratings (60Hz), aNSI Standard.

[5] D. Fischer, A. H¨artl, and B. Wille-Haussmann, "Model for electric load profiles with high time resolution for german households," Energy and Buildings, vol. 92, pp. 170–179, 2015.

[6] J. Widén, A. M. Nilsson, and E. Wäckelgård, "A combined Markov-chain and bottom-up approach to modelling of domestic lighting demand," Energy and Buildings, vol. 41, no. 10, pp. 1001-1012, 2009.

[7] W.H. Press, S.A. Teukolsky, W.T. Vetterling, B.P. Flannery, "Digital Filtering in the Time Domain" in *Numerical Recipes in Fortran*, 2nd ed. Cambridge , England: CUP, 1986-1992, ch.13, sec. 5, pp. 551-556

[8] "Chapter 9 – Interfacing with External Software" http://gridlab-d.shoutwiki.com/wiki/Chapter_9_-_Interfacing_with_External_Software, accessed: 2017-08-18.

[9] "FNCS-Tutorial/demo-large/" https://github.com/GridOPTICS/FNCS-Tutorial/tree/master/demo-large, accessed: 2017-08-20.